The Plant Cell, Vol. 22: 1249–1263, April 2010, www.plantcell.org

VND-INTERACTING2, a NAC Domain Transcription Factor, Negatively Regulates Xylem Vessel Formation in *Arabidopsis* [W] [OA]

Masatoshi Yamaguchi,[a,b] Misato Ohtani,[a,c] Nobutaka Mitsuda,[d] Minoru Kubo,[a,1] Masaru Ohme-Takagi,[d] Hiroo Fukuda,[e] and Taku Demura[a,b,c,2]

[a] RIKEN Plant Science Center, Yokohama, Kanagawa 230-0045, Japan
[b] Graduate School of Biological Sciences, Nara Institute of Science and Technology, Ikoma, Nara 630-0192, Japan
[c] RIKEN Biomass Engineering Program, Yokohama, Kanagawa 230-0045, Japan
[d] Research Institute of Genome-Based Biofactory, National Insitute of Advanced Industrial Science and Technology, Tsukuba, Ibaraki 305-8562, Japan
[e] Department of Biological Sciences, Graduate School of Science, University of Tokyo, Tokyo 113-0033, Japan

The *Arabidopsis thaliana* NAC domain transcription factor VASCULAR-RELATED NAC-DOMAIN7 (VND7) acts as a master regulator of xylem vessel differentiation. To understand the mechanism by which VND7 regulates xylem vessel differentiation, we used a yeast two-hybrid system to screen for proteins that interact with VND7 and identified cDNAs encoding two NAC domain proteins, VND-INTERACTING1 (VNI1) and VNI2. Binding assays demonstrated that VNI2 effectively interacts with VND7 and the VND family proteins, VND1-5, as well as with other NAC domain proteins at lower affinity. *VNI2* is expressed in both xylem and phloem cells in roots and inflorescence stems. The expression of *VNI2* overlaps with that of *VND7* in elongating vessel precursors in roots. VNI2 contains a predicted PEST motif and a C-terminally truncated VNI2 protein, which lacks part of the PEST motif, is more stable than full-length VNI2. Transient reporter assays showed that VNI2 is a transcriptional repressor and can repress the expression of vessel-specific genes regulated by VND7. Expression of C-terminally truncated VNI2 under the control of the *VND7* promoter inhibited the normal development of xylem vessels in roots and aerial organs. These data suggest that VNI2 regulates xylem cell specification as a transcriptional repressor that interacts with VND proteins and possibly also with other NAC domain proteins.

INTRODUCTION

The plant vascular system, transporting water and nutrients and supporting the plant body, consists of the xylem and phloem, which differentiate from the vascular cambium and procambium. The xylem is composed of water-conducting vessel elements, supportive fibers, and xylem parenchyma cells, whereas the phloem comprises sugar-conducting sieve elements, accompanying companion cells, and phloem parenchyma cells.

Previous studies have identified a variety of signal molecules that govern vascular development and vascular cell specification: auxin (Scarpella et al., 2004), cytokinin (Mähönen et al., 2000, 2006; Yokoyama et al., 2007), brassinosteroid (Yamamoto et al., 1997; Caño-Delgado et al., 2004; Zhou et al., 2004), a proteoglycan-like factor called xylogen (Motose et al., 2004), CLAVATA3/ENDOSPERM SURROUNDING REGION-related (CLE) dodecapeptides called tracheary element differentiation inhibitory factors (TDIFs; Ito et al., 2006), and spermine (Muñiz et al., 2008). The negative regulation of protoxylem vessel differentiation by authentic His kinase–dependent cytokinin signaling was demonstrated in a mutant of *ARABIDOPSIS* HISTIDINE PHOSPHOTRANSFER PROTEIN6 (Mähönen et al., 2006) and a double mutant of *ARABIDOPSIS* RESPONSE REGULATOR 10 (ARR10) and ARR12 (Yokoyama et al., 2007). Xylogen and TDIF were identified with a bioassay of a zinnia (*Zinnia elegans*) xylogenic suspension culture system as extracellular factors enhancing and inhibiting vessel element differentiation, respectively (Motose et al., 2004; Ito et al., 2006). Mutation of ACAULIS5, a putative spermine synthase (Hanzawa et al., 2000), caused changes in the secondary wall patterning of the xylem vessel elements (Muñiz et al., 2008).

Several lines of genetic evidence also indicate that fate determination of the xylem and phloem and cell-type specification in each tissue are largely regulated by a number of transcription factors (reviewed in Carlsbecker and Helariutta, 2005; Sieburth and Deyholos, 2006; Demura and Fukuda, 2007; Turner et al., 2007). Analysis of loss- and gain-of-function phenotypes of the class III homeodomain–leucine zipper transcription factor (HD-Zip III) and GARP-type transcription factor KANADI (KAN)

[1] Current address: Hasebe Reprogramming Evolution Project, ERATO, Japan Science and Technology Agency, Okazaki, Aichi 444-8585, Japan.
[2] Address correspondence to demura@bs.naist.jp.
The author responsible for distribution of materials integral to the findings presented in this article in accordance with the policy described in the Instructions for Authors (www.plantcell.org) is: Taku Demura (demura@bs.naist.jp).
[W] Online version contains Web-only data.
[OA] Open Access articles can be viewed online without a subscription.
www.plantcell.org/cgi/doi/10.1105/tpc.108.064048

family members suggested that xylem/phloem determination is regulated by the antagonistic and complementary activities of the HD-Zip III and *KAN* gene products (Hawker and Bowman, 2004). A mutation in ALTERED PHLOEM DEVELOPMENT (APL), a MYB coiled-coil transcription factor, resulted in seedling lethality with defects in phloem-specific cell division and in sieve element differentiation in the roots, where ectopic differentiation of vessel elements occurred instead of the differentiation of sieve elements. However, *APL* overexpression prevents or delays vessel element formation, suggesting that APL is required for sieve element differentiation and to inhibit xylem differentiation (Bonke et al., 2003). Specification into distinctive xylem cells is regulated by several NAM/ATAF/CUC (NAC) domain transcription factors. *VASCULAR-RELATED NAC-DOMAIN1* (*VND1*) to *VND7* are preferentially expressed in differentiating xylem vessels (Kubo et al., 2005; Yamaguchi et al., 2008), and the overexpression of *VND7* and *VND6* can induce the ectopic differentiation of two different types of vessel elements: protoxylem vessels, typically with annular or spiral secondary wall thickenings, and metaxylem vessels, typically with reticulate or pitted secondary wall thickenings (Kubo et al., 2005). The functional suppression of VND7 and VND6 results in the inhibition of vessel element formation (Kubo et al., 2005; Yamaguchi et al., 2008). These results strongly suggest that VND6 and VND7 act as the key regulators of the differentiation of xylem vessels. *NAC SECONDARY WALL THICKENING PROMOTING FACTOR1* (*NST1*) and *NST3* (also called *SECONDARY WALL-ASSOCIATED NAC DOMAIN PROTEIN1* [*SND1*] or *ARABIDOPSIS NAC DOMAIN CONTAINING PROTEIN012* [*ANAC012*]) are expressed in the interfascicular fibers and xylem fibers and function redundantly in regulating secondary wall biosynthesis in fibers (Zhong et al., 2006, 2007b; Ko et al., 2007; Mitsuda et al., 2007). The gene encoding *XYLEM NAC DOMAIN1* (*XND1*) is highly expressed in xylem (Zhao et al., 2005), and its overexpression causes extreme dwarfism associated with the complete suppression of vessel secondary wall biosynthesis and programmed cell death, suggesting that XND1 negatively regulates xylem vessel differentiation (Zhao et al., 2008). SND2, MYB46, MYB103, and KNOTTED1-LIKE HOMEODOMAIN PROTEIN7 transcription factors are direct targets of NST3/SND1/ANAC012 and possibly of NST1, VND6, and VND7 (Zhong et al., 2007a, 2008), suggesting the existence of a transcriptional network regulating xylem differentiation.

A number of NAC domain transcription factors from several plant species play critical roles in diverse processes in addition to xylem cell specification, such as the establishment of the shoot apical meristem, lateral root formation, flowering time, senescence, abiotic stress responses, and defense responses (Delessert et al., 2005; Uauy et al., 2006; Yoo et al., 2007; Kim et al., 2008; Ogo et al., 2008; reviewed in Olsen et al., 2005). Recent analyses of the NAC genes have suggested that NAC function is regulated at the transcriptional, posttranscriptional, and posttranslational levels (reviewed in Olsen et al., 2005). Their posttranslational regulation via protein degradation may, as suggested by yeast two-hybrid screening, act through protein–protein interactions (Xie et al., 2002; Greve et al., 2003). VND7 can form homodimers and heterodimers with other VND proteins, and the stability of VND7 is regulated by proteasome-mediated degradation (Yamaguchi et al., 2008), suggesting that the transcriptional activity of VND7 is regulated by its interactions with other proteins.

In this study, to understand the mechanism by which xylem vessel differentiation is regulated, we used a yeast two-hybrid system to identify proteins that interact with VND7, which resulted in the isolation of a previously uncharacterized NAC domain transcription factor, VND-INTERACTING2 (VNI2). We show that VNI2 binds with high affinity to VND7 as well as to VND1 to VND5 proteins and with low affinity to some other NAC domain proteins and that *VNI2* is expressed in immature xylem cells and vessel precursors. We also show that VNI2 is a transcriptional repressor whose stability is regulated by PEST motif-dependent proteolysis and that it suppresses the capacity of VND7 to activate transcription. Moreover, the misexpression of *VNI2* under the control of the *VND7* promoter causes strong repression of xylem vessel differentiation. Considered together, our findings indicate that VNI2 regulates xylem cell specification as a transcriptional repressor that interacts with VND proteins and possibly with other NAC domain proteins.

RESULTS

VNI2 Encodes a Novel NAC Domain Protein that Interacts with VND7

The *Arabidopsis thaliana* NAC domain transcription factor VND7 acts as a master regulator of xylem vessel differentiation (Kubo et al., 2005; Yamaguchi et al., 2008). To further understand the mechanism by which VND7 regulates xylem vessel differentiation, we screened an *Arabidopsis* root cDNA library for proteins that interact with VND7, using a yeast two-hybrid system (Figure 1). Because full-length VND7 is a strong transcriptional activator in yeast (Yamaguchi et al., 2008), the N-terminal region of VND7 (amino acid residues 1 to 146), containing consensus subdomains I to IV of the NAC domain, was used as the bait for screening (Figure 1B). After screening more than 1.5×10^6 independent transformants, we identified eight positive clones with the expression of reporter genes (Figure 1A). Six and two cDNAs rescued from these clones encoded two distinct NAC domain proteins, ANAC082 and ANAC083, which were designated VNI1 and VNI2, respectively (Figure 1; see Supplemental Figure 1A online). All the rescued *VNI1* cDNAs lacked a part of the NAC domain but contained the putative C-terminal transcriptional activation domain, which included a possible PEST proteolysis target motif (PEST score of +7.17; Rechsteiner and Rogers, 1996) and nine tandemly repeated sequences of 13 amino acids (see Supplemental Figure 1B online). Both *VNI2* cDNAs included NAC subdomain V and the C-terminal transcriptional activation domain (amino acid residues 147 to 252), containing a possible PEST motif (amino acid residues 213 to 226, TTDLNLLPSSPSSD; PEST score of +4.87; Rechsteiner and Rogers, 1996; Figure 1B). Because our previous transcriptome data showed that *VNI2* expression is significantly upregulated during in vitro vessel element transdifferentiation in *Arabidopsis* suspension cells (Figure 1D; Kubo et al., 2005), whereas *VNI1* expression was not related to vessel element differentiation (see Supplemental Figures 1C and 1D online), we decided to focus on the functional analysis of VNI2 in this study.

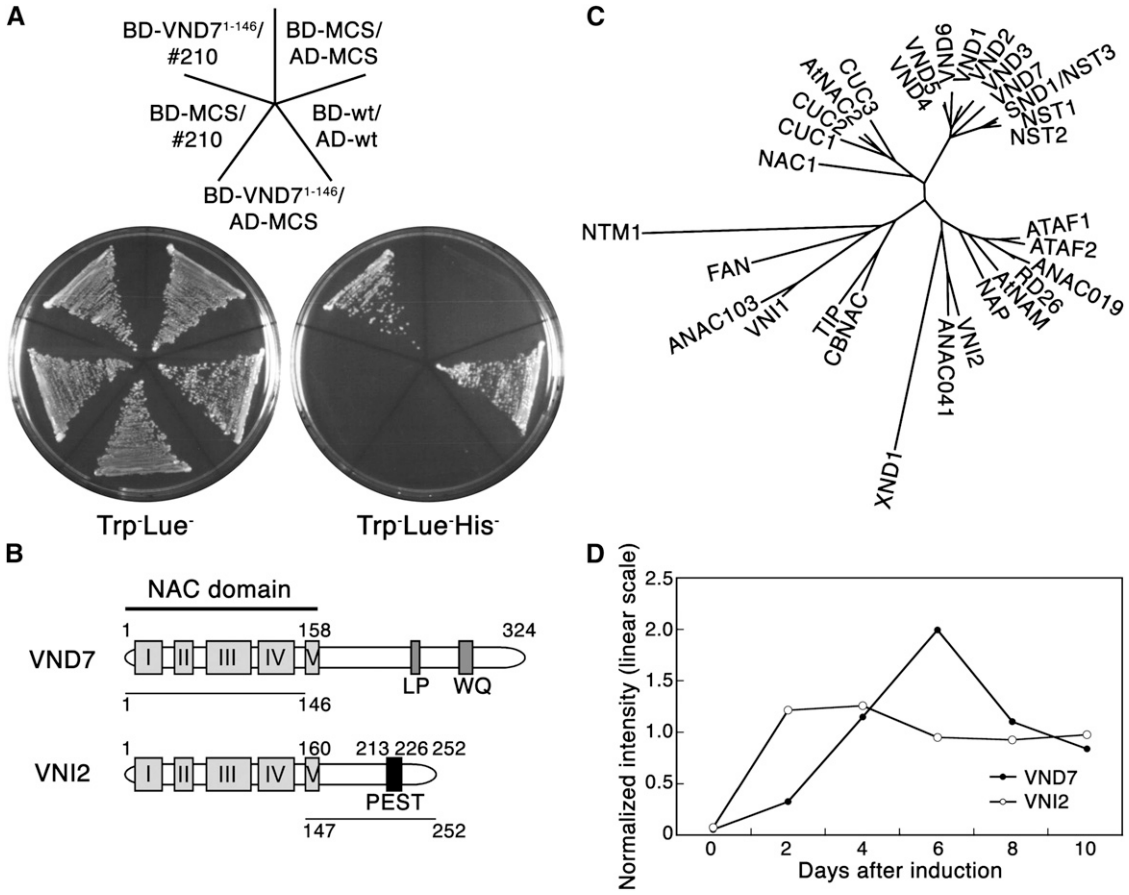

Figure 1. Identification of VNI2 as a Protein that Interacts with VND7.

(A) Interaction between VNI2 and VND7 in yeast cells. Yeast cells carrying plasmids containing amino acid residues 1 to 146 of VND7 fused to GAL4-BD (BD-VND7$^{1-146}$) and amino acid residues 147 to 221 of VNI2 fused to GAL4-AD (#210), which was isolated by yeast two-hybrid screening, grew on selective medium lacking Trp, Leu, and His. Plasmids containing a multicloning site (MCS) fused to GAL4-BD or GAL4-AD were used as the negative controls, and pBD-wt and pAD-wt (Stratagene) were used as the positive controls.

(B) Schematic structure of the VND7 and VNI2 proteins. The NAC domain, which contains subdomains I to V, is conserved at the N termini of the VND7 and VNI2 proteins. LP and WQ represent the LP and WQ boxes conserved in the IIb/OsNAC7 subgroup (Ko et al., 2007). VNI2 has a predicted PEST motif in the C-terminal region. Amino acid residues 1 to 146 of VND7, used as the bait, and residues 147 to 221 of VNI2, obtained by screening, are shown below each protein.

(C) Phylogenetic analysis of VNI1, VNI2, and other previously characterized *Arabidopsis* NAC domain proteins.

(D) Expression patterns of *VND7* and *VNI2* genes during in vitro vessel element transdifferentiation in *Arabidopsis* suspension cells, as determined by microarray analysis (Kubo et al., 2005).

VNI2 Interacts with VND proteins in Vitro

To confirm the interaction between VND7 and VNI2, we performed in vitro binding assays with poly-His-tagged VNI2 (His-VNI2) expressed in *Escherichia coli* and immobilized on Ni-conjugated agarose resin, and with several NAC domain proteins, including VND7, prepared in a rabbit reticulocyte lysate system in the presence of [^{35}S]Met. Proteins bound to the resin were separated by SDS-PAGE and detected by autoradiography; a mock-treated control lacking His-VNI2 showed no [^{35}S]Met-labeled proteins (Figure 2A). Although all the NAC domain proteins bound to the His-VNI2 resin to some extent, VND7, VND1, VND2, and VND3 bound more efficiently than other NAC proteins, including VND6 and NAC1 (Xie et al., 2000), CUP-SHAPED COTYLEDON2 (CUC2; Aida et al., 1997), and VNI2 (Figure 2A). Because VND4 and VND5 bound nonspecifically to the Ni-conjugated agarose resin, the binding capacity of VND4, VND5, and VND7 was confirmed with VNI2 fused to maltose binding protein (MBP-VNI2) immobilized on amylose resin (see Supplemental Figure 2 online). We further tested the binding specificity between VND7 and VNI2 using MBP fused to ANAC041, which has the highest sequence similarity to VNI2 (Figure 1C; see Supplemental Data Set 1 online), as a reference, and found that VND7 selectively bound to VNI2 rather than to ANAC041 (Figure 2B). These results demonstrate that VND7 and other VND proteins, VND1 to VND5, preferentially bind to VNI2 with moderate specificity.

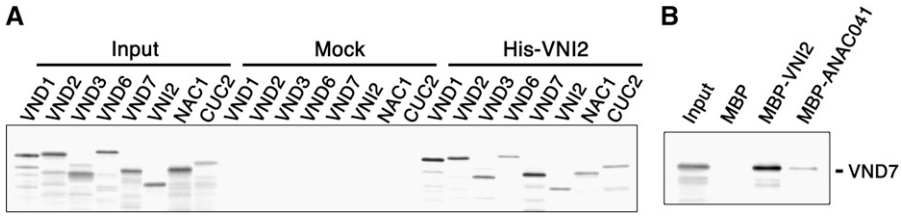

Figure 2. In Vitro Binding of VNI2 to NAC Domain Proteins.

(A) VNI2 effectively interacts with VND7. [^{35}S]Met-labeled NAC domain proteins (Input) were incubated with Ni-agarose conjugated with poly-His-tagged VNI2 (His-VNI2) or with Ni-agarose only (Mock). Proteins bound to the beads were visualized by SDS-PAGE and autoradiography. One-quarter of the translation product is included as a control (Input).

(B) VND7 interacts with VNI2 with much higher affinity than with ANAC041. [^{35}S]Met-labeled VND7 was incubated with amylase resin beads conjugated with MBP-VNI2, MBP-ANAC041, or MBP. Proteins bound to the beads were visualized by SDS-PAGE and autoradiography.

VNI2 Is Expressed in Both Xylem and Phloem Cells in Roots and Inflorescence Stems

The developmental expression profile of *VNI2* was investigated in transgenic *Arabidopsis* plants by expressing, under the *VNI2* promoter (*VNI2*$_{pro}$), reporter genes encoding yellow or cyan fluorescent protein (YFP or CFP, respectively) fused to the SV40 nuclear localization signal (NLS) or β-glucuronidase (GUS). Expression at the cellular level during root development was determined with *VNI2*$_{pro}$*:YFP-NLS* and *VNI2*$_{pro}$*:CFP-NLS* (Figures 3A and 3C; see Supplemental Figure 3A online). *VNI2* expression was first detected in several cell files within the meristematic procambial region at the root tip (Figures 3A and 3C), which are closely associated with the early development of the protophloem. *VNI2* expression partially overlapped with and preceded the expression of the phloem-specific *APL* gene (Bonke et al., 2003) in transgenic *Arabidopsis* roots expressing *VNI2*$_{pro}$*:CFP-NLS* and *APL*$_{pro}$*:YFP-NLS* together (see Supplemental Figure 3A online). *VNI2* expression was also detected in the protoxylem poles, from the upper edge of the root meristem to the elongation zone (Figures 3A and 3C), which were located perpendicular to the protophloem poles (Figures 3A and 3C). The accumulation of *VNI2* mRNA in both protophloem and protoxylem cells was also detected by in situ hybridization (see Supplemental Figures 3B and 3C online). In the more distal part of the root, *VNI2* was expressed in various cells of the central cylinder (Figures 3A; see Supplemental Figure 4 online). In the aerial parts of the plant, *VNI2* was also preferentially expressed in vascular cells, including the xylem parenchyma cells surrounding the mature vessel elements and several phloem cells in the inflorescence stems, and in guard cells in the leaves (Figures 3E to 3G). *VND7* was also expressed in vascular cells in *Arabidopsis* seedlings (Yamaguchi et al., 2008). To examine the cells in which the expression of *VNI2* and *VND7* overlapped, we generated transgenic plants carrying *VND7*$_{pro}$*:YFP-NLS* (Figures 3B and 3D), *VND7*$_{pro}$*:YFP-NLS*, and *VNI2*$_{pro}$*:CFP-NLS* together (see Supplemental Figure 4 online) and *VND7*$_{pro}$*:GUS* (see Supplemental Figure 5 online). As described by Kubo et al. (2005), *VND7* expression (YFP) was detected in the elongating protoxylem vessel precursors around a position just above the root meristem (Figure 3B; see Supplemental Figure 4 online), where *VNI2* expression was also detected (Figures 3A and 3C; see Supplemental Figure 4 online), demonstrating their overlapping expression in elongating protoxylem vessel precursors. However, *VNI2* expression was detected in the vessel precursors before elongation, whereas only *VND7* was expressed at later stages in the elongating protoxylem vessel precursors (see Supplemental Figure 4 online). This overlapping expression was also observed in the metaxylem vessel precursors in the developed parts of the roots, where only *VND7* was expressed in the differentiating protoxylem vessels with patterned secondary cell walls (Figures 3B and 3D; see Supplemental Figure 4 online). These data suggest that *VNI2* expression precedes *VND7* expression during xylem vessel differentiation. Expression of *VNI2* and *VND7* was also evident in the nonvessel cells of the root central cylinder (Figure 3A; Yamaguchi et al., 2008) and in the xylem parenchyma cells as well as differentiating xylem cells in the inflorescence stem (Figure 3G; see Supplemental Figure 5 online), suggesting a cooperative function of VND7 and VNI2 even in these nonvessel cells.

VNI2 Stability Is Regulated by the PEST Motif

Transgenic *Arabidopsis* plants expressing full-length *VNI2* fused to a *GUS* reporter gene (*VNI2*^{full}*-GUS*) under the control of *VNI2*$_{pro}$ were prepared to localize *VNI2* expression more precisely. GUS staining was faint in the roots (Figure 4A) and hardly detectable in the shoots (Figure 4C), which differed from the GUS staining pattern in the *VNI2*$_{pro}$*:GUS* seedlings (Figure 3), suggesting the degradation of the VNI2-GUS fusion protein in the *VNI2*$_{pro}$*:VNI2*^{full}*-GUS* seedlings. Because VNI2 has a possible PEST motif in the C-terminal region (Figure 1), we investigated whether this motif plays a role in the degradation of VNI2-GUS. We generated transgenic *Arabidopsis* plants expressing truncated VNI2 (amino acid residues 1 to 221), which lacked a portion of the C-terminal region containing about half the PEST motif sequence (Figure 1B) and was fused to the *GUS* reporter gene under the control of *VNI2*$_{pro}$ (*VNI2*$_{pro}$*:VNI2*$^{1-221}$*-GUS*). All the *VNI2*$_{pro}$*:VNI2*$^{1-221}$*-GUS* seedlings analyzed showed stronger GUS staining in the roots (Figure 4B) and visible GUS staining in the shoots, including in the shoot apical region (Figure 4D), compared with that in the *VNI2*$_{pro}$*:VNI2*^{full}*-GUS* seedlings. Consistent with microscopy observations, GUS activity was higher in

the *VNI2*$_{pro}$*:VNI2*$^{1-221}$*-GUS* plants than in the *VNI2*$_{pro}$*:VNI2*^{full}*-GUS* plants (Figure 4E). Furthermore, the *VNI2*$_{pro}$*:VNI2*^{full}*-GUS* seedlings treated with MG-132, a proteasome inhibitor, displayed higher GUS activity than seedlings treated with DMSO (Figure 4F). These data suggest that the stability of VNI2 is regulated by proteasome-mediated proteolysis and that the C-terminal region of the VNI2 protein, containing a possible PEST motif, is involved in maintaining the stability of VNI2.

VNI2 Is a Transcriptional Repressor

Most NAC domain proteins have been characterized as transcriptional activators (reviewed in Olsen et al., 2005). To examine

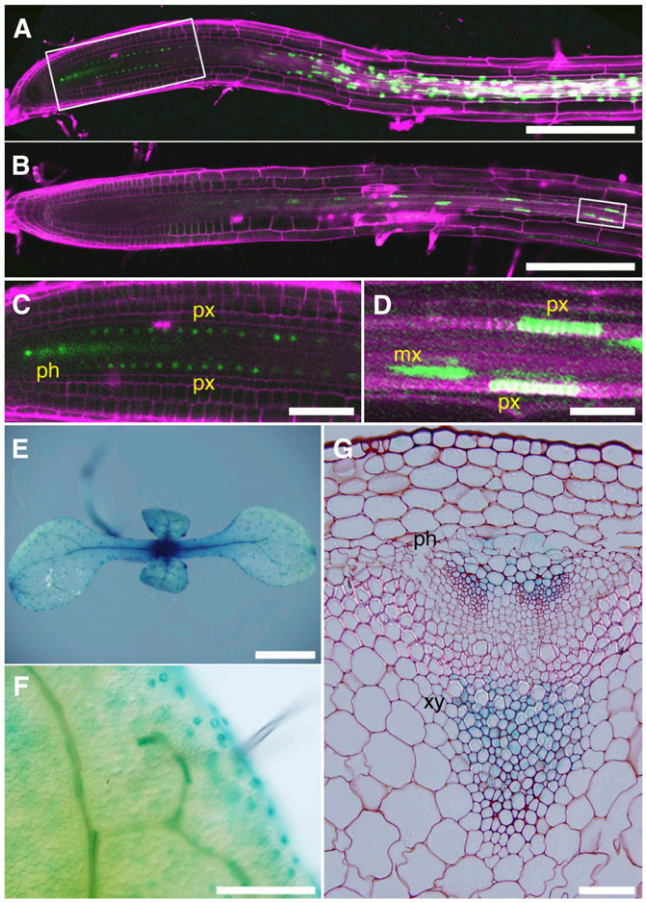

Figure 3. Expression Patterns of *VNI2*.

(A) to **(D)** Expression of *VNI2*$_{pro}$*:YFP-NLS* (**[A]** and [**C**]) and *VND7*$_{pro}$*:YFP-NLS* (**[B]** and [**D**]) in the roots. Confocal laser scanning microscopy images of roots counterstained with propidium iodide (magenta). **(C)** and **(D)** show magnified views of the region indicated by the white frames in **(A)** and **(B)**, respectively. mx, metaxylem; ph, phloem; px, protoxylem. Bars = 200 μm in **(A)** and **(B)**, 50 μm in **(C)**, and 20 μm in **(D)**.
(E) and **(F)** Expression of *VNI2*$_{pro}$*:GUS* in 7-d-old seedlings. Bars = 1 mm in **(E)** and 200 μm in **(F)**.
(G) Expression of *VNI2*$_{pro}$*:GUS* in the inflorescence stems of 6-week-old plants. A 5-μm section of the stem was counterstained with neutral red. ph, phloem; xy, xylem. Bar = 50 μm.

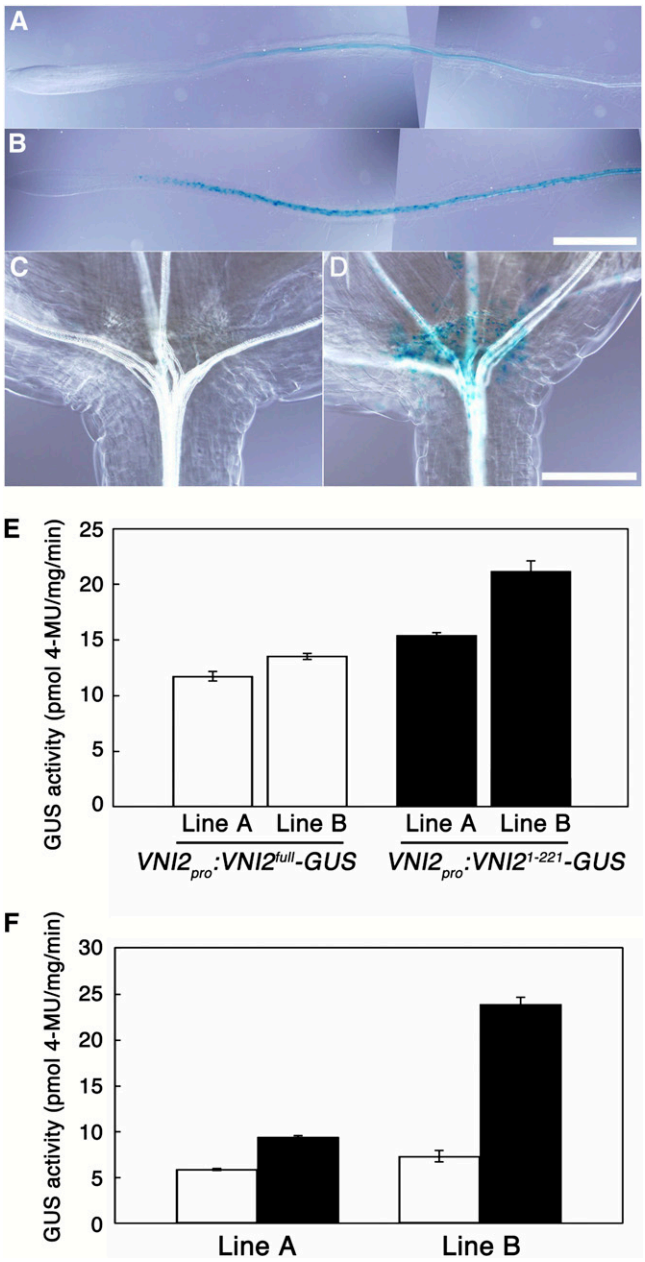

Figure 4. Stability of VNI2 Is Regulated by Protein Degradation.

(A) and **(B)** GUS staining of roots in transgenic plants carrying *VNI2*$_{pro}$*:VNI2*^{full}*-GUS* **(A)** or *VNI2*$_{pro}$*:VNI2*$^{1-221}$*-GUS* **(B)**, which lacks a portion of the C-terminal region containing about half of the PEST motif sequence. Bar = 500 μm.
(C) and **(D)** GUS staining of the shoot apical regions in transgenic plants carrying *VNI2*$_{pro}$*:VNI2*^{full}*-GUS* **(C)** and *VNI2*$_{pro}$*:VNI2*$^{1-221}$*-GUS* **(D)**. Bar = 200 μm.
(E) GUS activities of 8-d-old *VNI2*$_{pro}$*:VNI2*^{full}*-GUS* and *VNI2*$_{pro}$*:VNI2*$^{1-221}$*-GUS* plants. Two independent T3 generation lines were tested. Error bars indicate SD (n = 3).
(F) GUS activities of 7-d-old *VNI2*$_{pro}$*:VNI2*^{full}*-GUS* plants. Two independent T3 generation lines were tested. Closed and open bars indicate GUS activities of cells treated with MG-132 and DMSO for 6 h, respectively. Error bars indicate SD (n = 3).

the transcriptional function of VNI2, we used transient reporter assays (Figure 5). A reporter plasmid containing firefly *luc* linked to GAL4 binding sites, and effector plasmids containing *VND7*, *VNI2*^{full}, or *VNI2*$^{1-221}$ fused to *GAL4-BD* under the control of the cauliflower mosaic virus (*CaMV*) *35S* promoter (*35S*$_{pro}$), were delivered into *Arabidopsis* leaves by particle bombardment (Figure 5A). Although an increase of more than fourfold in Luc activity was induced by the expression of *GAL4-BD-VND7* compared with that induced by the *GAL4-BD* control, as reported previously (Yamaguchi et al., 2008), GAL4-BD-VNI2^{full} did not induce this increase in Luc activity (Figure 5B), suggesting that VNI2 is not a transcriptional activator. However, it remained possible that the unstable nature of VNI2 led to the low level of Luc activity. Therefore, we examined Luc activity after the expression of the possibly more stable derivative, GAL4-BD-VNI2$^{1-221}$; however, this did not enhance Luc activity (Figure 5B). These data prompted us to examine whether VNI2 has transcriptional repression activity. We used *luc* under the control of *35S*$_{pro}$, with GAL4 binding sites to increase the basal Luc activity (Mitsuda et al., 2005), as the reporter plasmid (Figure 5A), which was delivered into *Arabidopsis* leaves with the effector plasmids. As expected, GAL4-BD fused to the SRDX strong repression domain (Hiratsu et al., 2002) severely reduced the relative Luc activity compared with that of the GAL4-BD control (to <10% of the control), and GAL4-BD-VNI2^{full} and -VNI2$^{1-221}$ significantly reduced the Luc activity (to ~40 to 60% of the control; Figure 5C). Taking these results together, we conclude that VNI2 is a transcriptional repressor and that the potential repression-related sequence of VNI2 is located between amino acid residues 1 and 221, upstream of the possible PEST motif.

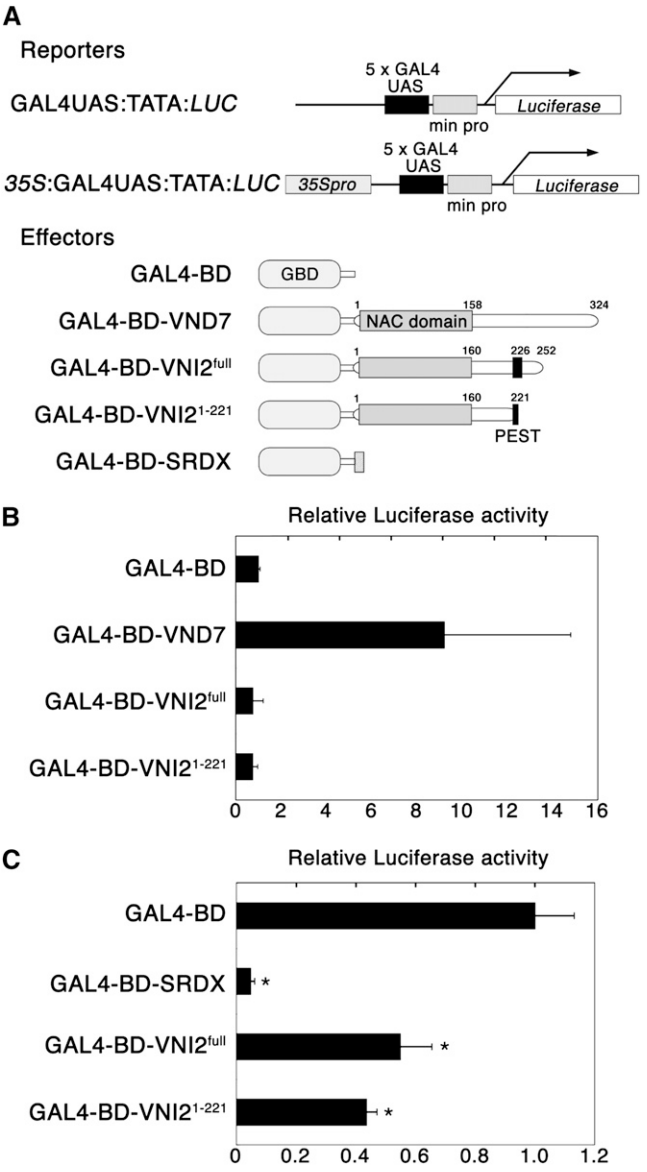

Figure 5. VNI2 Acts as a Transcriptional Repressor.

(A) Schematic diagrams of the effector and reporter constructs. The reporter construct contains repeated GAL4 binding sites (5 × GAL4 upstream activation sequence [UAS]) and a minimal *CaMV 35S* promoter (min pro) upstream from the firefly luciferase reporter gene, with or without the enhancer region of the *CaMV 35S* promoter (*35Spro*): GAL4UAS:TATA*:LUC* or GAL4UAS:TATA*:LUC*, respectively. The effector constructs encode VND7, full-length or C-terminally truncated VNI2, or the strong repression domain SRDX fused to the GAL4 DNA binding domain (GBD) downstream from the *CaMV35S* promoter.

(B) and **(C)** Relative luciferase activities after cobombardment of one of the effector constructs with GAL4UAS:TATA*:LUC* **(B)** or *35Spro*: GAL4UAS:TATA*:LUC* **(C)**. The reporter gene activity was normalized to the activity of *Renilla* luciferase, the gene that was cobombarded as a reference. Error bars indicate SD (n = 3 or 6). Asterisks indicate statistically significant differences ($P < 0.05$) relative to GAL4-BD.

Overexpression of *VNI2* Causes Defects in Vessel Formation

To examine whether VNI2 is involved in the development of xylem tissues, we generated transgenic *Arabidopsis* plants overexpressing *VNI2* or *VNI2-SRDX* under the control of *35S*$_{pro}$. *35S*$_{pro}$*:VNI2* seedlings of the T1 generation showed no clear differences from the control seedlings in appearance, whereas overexpression of *VNI2-SRDX* retarded the growth of the seedlings (10 of 42 lines) (Figure 6A). However, microscopy observations revealed defects in root vessel formation in the *35S*$_{pro}$*:VNI2* seedlings (13 of 31 lines) (Figures 6B to 6D). The control roots had two protoxylem vessels with helical secondary cell walls and three to four metaxylem vessels with reticulated secondary cell walls located between the protoxylem vessels in the mature region of the primary roots (Figure 6B). By contrast, the *35S*$_{pro}$*:VNI2* seedlings exhibited discontinuous vessel formation of one or both protoxylem vessel columns (Figures 6C and 6D). The same defect in vessel formation was observed when *VNI2-SRDX* was overexpressed (17 of 38 lines) (Figure 6E), indicating that the defects in protoxylem vessel formation in the *35S*$_{pro}$*:VNI2* seedlings were the result of the transcriptional repression activity of VNI2. Similar inhibition of vessel formation was previously shown by the overexpression of *VND7-SRDX* (Kubo et al., 2005) or C-terminally truncated *VND7* (Yamaguchi et al., 2008), suggesting a functional interaction between VNI2 and VND7.

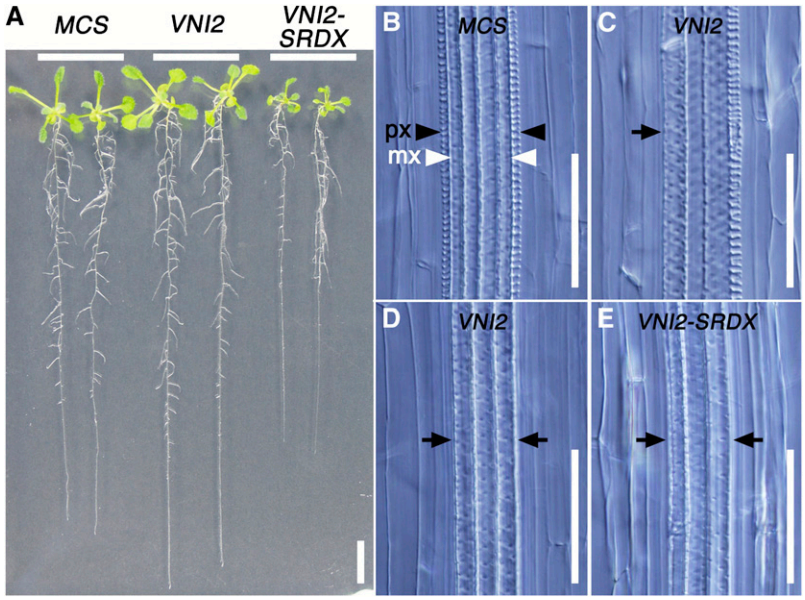

Figure 6. Overexpression of *VNI2* Inhibits Protoxylem Vessel Formation in Roots.

(A) Fourteen-day-old T1 seedlings carrying $35S_{pro}$*:MCS* (left two plants), $35S_{pro}$*:VNI2* (middle two plants), or $35S_{pro}$*:VNI2-SRDX* (right two plants). Bars = 1 cm.

(B) Xylem vessel formation in the roots of 14-d-old control plants ($35S_{pro}$*:MCS*). In the central region of the primary roots of the control plants, two protoxylem vessel cells (black arrowheads, px) were formed continuously, between which four metaxylem vessel cells (white arrowheads, mx) were located. Bar = 50 μm.

(C) to **(E)** Xylem vessel formation in roots of 14-d-old seedlings overexpressing *VNI2* (**[C]** and [**D**]) or *VNI2-SRDX* **(E)**. Black arrows indicate the absence of vessels on one side **(C)** or both sides (**[D]** and [**E**]) of the protoxylem vessel columns in the roots. Bars = 50 μm.

To further substantiate this functional interaction, we generated transgenic *Arabidopsis* plants expressing *VNI2* under the control of $VND7_{pro}$, which extends the *VNI2* expression to the differentiating vessel elements at later stages. Among 28 first-generation transgenic plants carrying $VND7_{pro}$:$VNI2^{full}$, nine grew more slowly than control plants carrying $VNI2_{pro}$:$VNI2^{full}$. These slow-growing plants had an apparent defect in vessels, exhibiting discontinuous vessel formation in root proto- and metaxylem (Figures 7A to 7C; see Supplemental Figure 6 online). Because C-terminally truncated VNI2 ($VNI2^{1-221}$) is more stable than full-length VNI2, it is likely that the expression of truncated *VNI2* effectively causes the vessel defect. Therefore, we also generated transgenic *Arabidopsis* plants expressing $VNI2^{1-221}$ under $VNI2_{pro}$ or $VND7_{pro}$. Although 30-d-old seedlings of the $VNI2_{pro}$:$VNI2^{1-221}$ plants (seven of 17 lines) showed slightly reduced growth, they grew and bolted normally thereafter (Figure 7A; see Supplemental Figure 6 online). The vessel defect was enhanced markedly in $VND7_{pro}$:$VNI2^{1-221}$ plants (17 of 38 lines), which often showed a severe dwarf phenotype with downward curled, dark-green rosette leaves and survived without bolting (Figure 7A; see Supplemental Figure 6 online). The dwarf seedlings also showed discontinuous vessel formation in their aerial parts (Figure 7E) as well as inhibited xylem vessel formation in their roots. These results demonstrate that the misexpression of *VNI2* (i.e., coexpression with *VND7* and the stabilization of VNI2 protein) leads to striking abnormalities in vessel formation.

A Number of Vessel-Specific Genes Are Regulated Downstream of VND7

It is plausible that VNI2 binds to VND7 and/or other VND family proteins and represses their transcriptional activation of downstream vessel-related genes. We previously demonstrated using promoter analysis that the expression of three immature vessel-specific genes, At *Xyn3*, *CesA7/IRX3*, and *LAC4/IRX12*, are upregulated downstream of VND7 (Kubo et al., 2005). To identify additional genes downstream of VND7, we performed a microarray experiment with the GeneChip ATH1 *Arabidopsis* genome array (Affymetrix, http://www.affymetrix.com/index.affx) in transgenic *Arabidopsis* roots overexpressing *YFP* and *VND7-YFP* under the control of $35S_{pro}$. Data analysis, including statistical Student's *t* test ($P < 0.05$) and false discovery rate ($Q < 0.05$), revealed 89 and 43 genes that were up- and downregulated at least fourfold, respectively, by *VND7-YFP* overexpression (see Supplemental Data Set 2 online). Forty-one of the upregulated genes, including *VND7*, were transiently expressed during in vitro vessel element transdifferentiation in *Arabidopsis* suspension cells (Table 1; Kubo et al., 2005). In addition to *VND7* itself, two other transcription factors were included among the 41 genes (Table 1). Expression of *LOB domain protein30* (*LBD30*)/*ASYMMETRIC LEAVES2 LIKE19* (*ASL19*)/*JAGGED LATERAL ORGANS* (*JLO*) is regulated by VND6 and VND7, and LBD30/ASL19/JLO seems to be involved in a positive feedback loop for *VND* expression (Soyano et al., 2008). *MYB46* is a direct target of

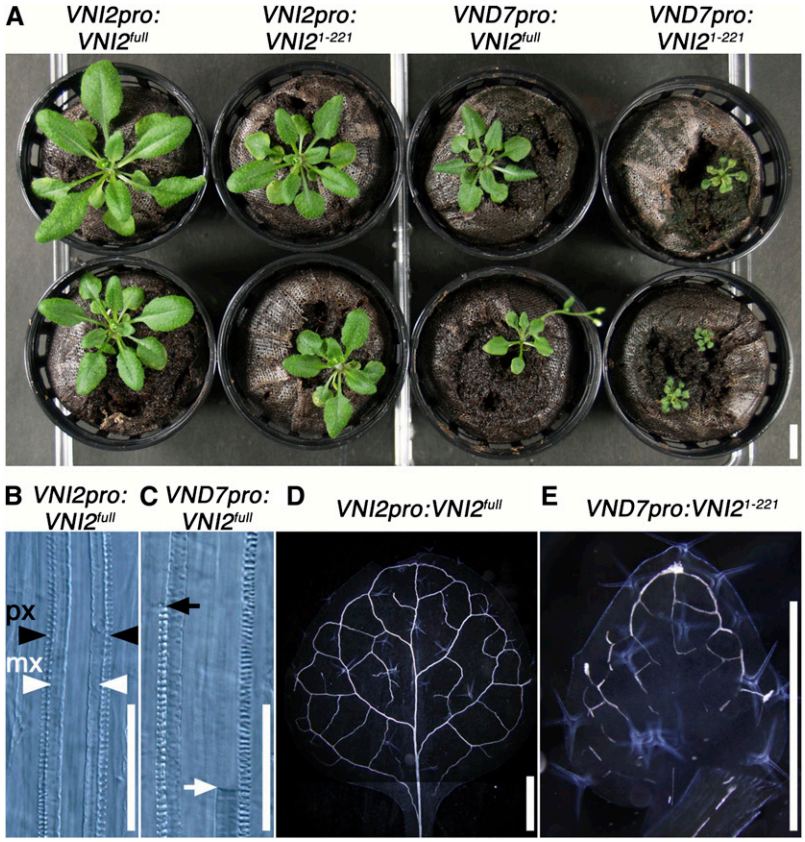

Figure 7. Expression of *VNI2* Driven by the *VND7* Promoter Caused Dwarfism and Vessel Defects.

(A) Thirty-day-old transgenic plants. From left to right, T1 generation transgenic plants carrying $VNI2_{pro}$:$VNI2^{full}$, $VNI2_{pro}$:$VNI2^{1–221}$, $VND7_{pro}$:$VNI2^{full}$, or $VND7_{pro}$:$VNI2^{1–221}$. Bar = 1 cm.

(B) and **(C)** Root phenotype of the $VNI2_{pro}$:$VNI2^{full}$ **(B)** and $VND7_{pro}$:$VNI2^{full}$ plants **(C)**. Black and white arrowheads in **(B)** indicate protoxylem and metaxylem vessels, respectively. Black and white arrows in **(C)** indicate the ends of discontinuous protoxylem and metaxylem vessels, respectively. Bars = 50 μm.

(D) and **(E)** Dark-field images of the first true leaves of 14-d-old T1 seedlings carrying $VNI2_{pro}$:$VNI2^{full}$ **(D)** or $VND7_{pro}$:$VNI2^{1–221}$ **(E)**. Bars = 1 mm.

NST3/SND1/ANAC012 and possibly of VND7 (Zhong et al., 2007a). Likewise, we found a number of genes previously shown to be associated with morphogenesis during vessel element differentiation: cellulose synthase subunits (*CesA4*/*IRX5*, *CesA7*/*IRX3*, and *CesA8*/*IRX1*; Taylor et al., 2003), a glycosylsyltransferase for xylan synthesis (*IRX9*; Brown et al., 2005), a laccase (*LAC4*/*IRX12*; Brown et al., 2005), a peroxidase (At *Prx66*; Sato et al., 2006), and a xylem cysteine protease (*XCP1*; Funk et al., 2002) (Table 1). Next, we checked for changes in the expression levels of previously described vascular-related genes (see Supplemental Data Set 3 online). Although no substantial changes were observed for genes associated with procambium formation or vascular pattern formation (such as the HD-Zip III and KAN families, the brassinosteroid receptors, or xylogens; Fukuda, 2004), the expression of a number of genes responsible for *IRX* mutations (*IRX1*, *-3*, *-5*, *-6*, *-8*, *-9*, *-10*, *-12*, and *-13*) and known vessel-specific genes (encoding a glycosyl hydrolase family 10 protein At Xyn3; aspartyl protease; XCP1 and XCP2; subtilisin-type serine protease XSP1; and At Prx66) were significantly upregulated (at least twofold; $P < 0.05$; $Q < 0.05$) by *VND7* overexpression.

We confirmed by quantitative RT-PCR that expression levels of *VND7*, *LBD30*/*ASL19*/*JLO*, *MYB46*, and *XCP1* were higher in the $35S_{pro}$:*VND7-YFP* plants than in the $35S_{pro}$:*YFP* plants, which was consistent with the GeneChip analysis data (see Supplemental Figure 8A online). We next investigated whether VND7 can activate the transcription of these vessel-specific genes in a transient Luc reporter assay system. *LBD30*/*ASL19*/*JLO*, *MYB46*, and *XCP1* were selected for the assay, and the promoter regions of these genes were linked to *luc* as reporter plasmids (Figure 8A), which were delivered into *Arabidopsis* leaves with an effector plasmid containing $35S_{pro}$ linked to *VND7* cDNA (Figure 8A). We demonstrated that VND7 effectively transactivated *luc* transcription via these three promoters (Figure 8B).

VNI2 Represses the Transcriptional Activation Activity of VND7

To investigate whether VNI2 is sufficient to repress the expression of vessel-specific genes that are transactivated by VND7, we generated effector plasmids containing $35S_{pro}$ linked to

Table 1. In Vitro Vessel Element Differentiation-Related Genes with Expression Changes of at Least Fourfold in *35S$_{pro}$:VND7-YFP* (VND7-YFP ox) Transgenic Plants ($P < 0.05$, $Q < 0.05$)

AGI No.	Description	Fold Change	P Value	Q Value
Transcription factors				
At4g00220	LBD30/ASL19/JLO	6.11	0.00003900	0.0078
At5g12870	At MYB46	5.97	0.00082000	0.0230
At1g71930	VND7	5.18	0.00002200	0.0065
Signal transduction				
At1g61610	Receptor-like kinase	8.85	0.00028000	0.0150
At1g55180	Phospholipase D ε	7.26	0.00010000	0.0110
At1g24030	Protein kinase family protein	4.76	0.00024000	0.0150
At1g01900	Subtilase family protein/At SBT1.1	4.64	0.00042000	0.0180
At1g54790	GDSL-motif lipase	4.62	0.00140000	0.0290
Cell wall				
At1g70500	Polygalacturonase, putative	12.40	0.00000230	0.0026
At5g07080	Transferase family protein	6.86	0.00012000	0.0110
At5g38610	Invertase/pectin methylesterase inhibitor family protein	6.67	0.00002100	0.0065
At3g52820	Purple acid phosphatase At PAP22	5.96	0.00000430	0.0027
At1g05310	Pectinesterase family protein	5.79	0.00003600	0.0078
At4g18780	Cellulose synthase CesA8/IRX1	5.64	0.00000110	0.0015
At5g44030	Cellulose synthase CesA4/IRX5	4.80	0.00002200	0.0065
At2g37090	Glycosyl transferase family 43/IRX9	4.44	0.00008100	0.0093
At5g17420	Cellulose synthase CesA7/IRX3	4.25	0.00000370	0.0027
At3g47400	Pectinesterase family protein	4.23	0.00004100	0.0078
At4g08160	Glycosyl hydrolase family 10/At Xyn3	4.03	0.00001700	0.0065
Lignification				
At5g03260	Laccase 11/LAC11	5.34	0.00003600	0.0078
At5g51890	Peroxidase /At Prx66/ZPO-C-like	4.26	0.00064000	0.0210
At2g38080	Laccase 4 /LAC4/IRX12	4.11	0.00010000	0.0100
Cell death				
At4g35350	Xylem Cys protease1/XCP1	5.78	0.00000058	0.0012
At5g04200	Metacaspase 9/ATMC9	4.77	0.00005600	0.0086
Unknown function				
At2g46760	FAD binding domain-containing	12.70	0.00001700	0.0065
At2g38320	Expressed protein	6.49	0.00004400	0.0078
At5g19870	Unknown protein	5.81	0.00006500	0.0086
At1g10800	Unknown protein	5.79	0.00000490	0.0028
At3g62020	Germin-like protein10/GLP10	5.63	0.00000097	0.0015
At2g34790	EDA28/MEE23	5.61	0.00026000	0.0150
At5g16490	RIC4	5.35	0.00000450	0.0027
At2g14095	Expressed protein	5.32	0.00002400	0.0066
At2g41610	Unknown protein	5.18	0.00008200	0.0093
At3g49070	Unknown protein	4.71	0.00005700	0.0086
At5g40020	Thaumatin family protein	4.47	0.00006200	0.0086
At4g18425	Expressed protein	4.47	0.00002100	0.0065
At5g01360	Putative protein	4.16	0.00002500	0.0066
At5g60720	Unknown protein	4.11	0.00003800	0.0078
At5g08480	VQ motif–containing protein	4.07	0.00036000	0.0170
At1g63300	Unknown protein	4.01	0.00210000	0.0340
At3g27200	Plastocyanin-like	4.00	0.00002200	0.0065

The fold changes (VND7-YFPox/YFPox) are calculated from normalized values; P values and Q values are given.

VNI2^{full} or *VNI2$^{1–221}$* cDNAs and delivered them into *Arabidopsis* leaves with reporter plasmids containing the promoters of *LBD30/ASL19/JLO*, *MYB46*, and *XCP1* (Figure 8A). We found that VNI2^{full} and VNI2$^{1–221}$, a possibly stable form of VNI2 (Figure 4), repressed *luc* expression transactivated by VND7 (Figure 8B), indicating that VNI2 functions as a repressor of the VND7-induced expression of vessel-specific genes. Quantitative RT-PCR revealed that the expression levels of *LBD30/ASL19/JLO* and *XCP1* were decreased in *VNI2$_{pro}$:VNI2$^{1-221}$* roots, which showed severe defects in xylem vessel formation (Figure 7) compared with the roots of control plants (see Supplemental Figure 8B online).

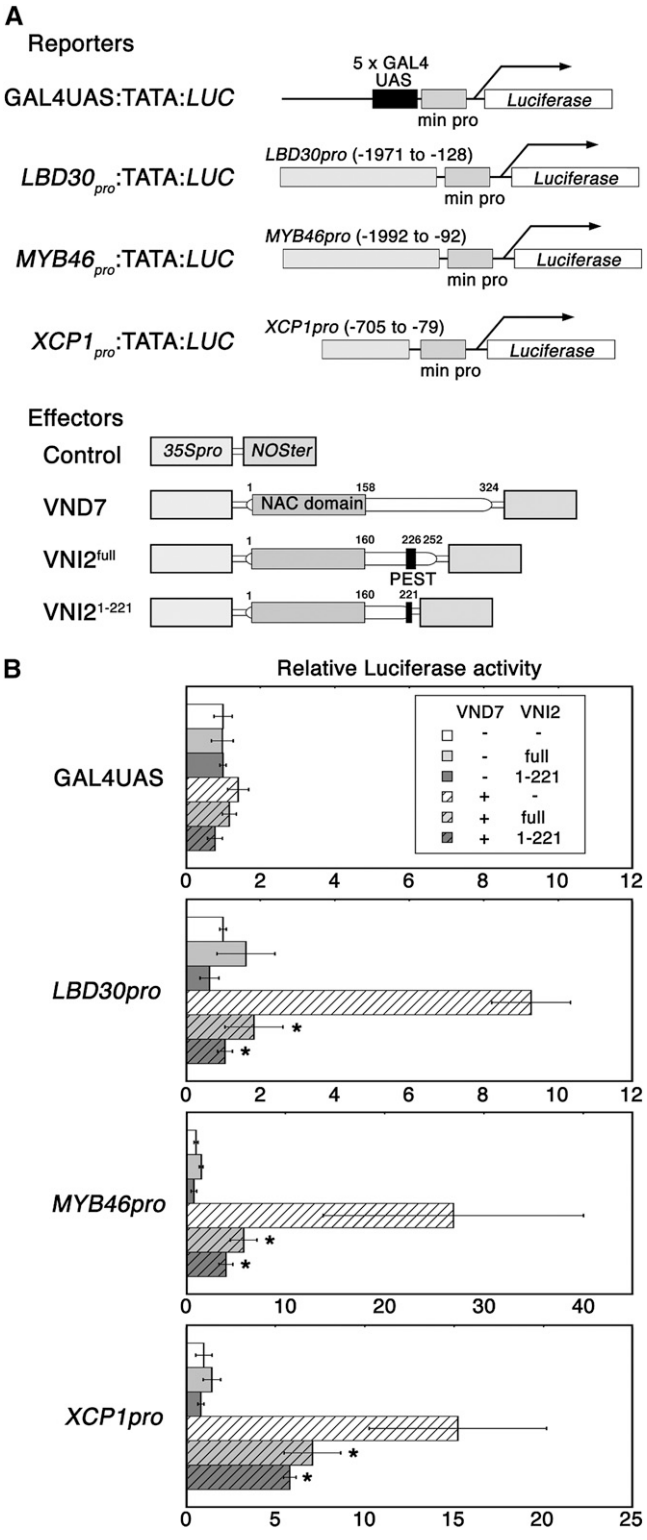

Figure 8. VNI2 Protein Inhibits the Transcriptional Activation Activity of VND7.

(A) Schematic diagrams of the effector and reporter constructs. The reporter construct contains the promoter of *LBD30/ASL19/JLO*, *MYB46*, or *XCP1* with a minimal *CaMV 35S* promoter (min pro) upstream from the firefly luciferase reporter gene. The effector constructs contained *VND7* or full-length or C-terminally truncated *VNI2* downstream from the *CaMV 35S* promoter.

(B) Relative luciferase activities after cobombardment of one of the reporter constructs with the effector constructs. The reporter gene activity was normalized to the activity of *Renilla* luciferase, which was cobombarded as a reference. Error bars indicate SD ($n = 3$). Asterisks indicate statistically significant differences ($P < 0.05$) from values for the *VND7* effector construct only.

The loss of VNI2 function was investigated with a T-DNA insertion line for *VNI2* (*vni2-1*, SALK_143793: T-DNA insertion immediately upstream of the coding region), and the level of *VNI2* transcripts was significantly reduced (see Supplemental Figure 7 online). Although the *vni2-1* mutant showed no visibly aberrant phenotype in terms of xylem vessel formation in roots, hypocotyls, and inflorescence stems, the expression levels of *LBD30/ASL19/JLO* and *XCP1* in *vni2-1* plants were increased compared with those of the wild type (see Supplemental Figure 7 online). These data suggested that VNI2 negatively regulates the expression of genes involved in xylem vessel formation.

DISCUSSION

VNI2 Is a Transcriptional Repressor

Most of the NAC domain transcription factors previously characterized are described as transcriptional activators based on assays in yeast and plant cells. However, a CALMODULIN BINDING NAC PROTEIN (CBNAC) was shown to act as a transcriptional repressor (Kim et al., 2007). Transcriptional repressors can be classified as passive or active repressors (reviewed in Thiel et al., 2004; Kazan, 2006). Our experiments suggested that VNI2 has features of both of these types of transcriptional repressor.

Passive repressors repress transcription either by competing with transcriptional activators for DNA binding, by interacting with transcriptional activators to form inactive heterodimers, or by binding to transcriptional coactivators to render transcriptional complexes inactive. The overexpression of C-terminally truncated VND7 protein, which lacks most of the transcriptional activation domain, exerts a dominant-negative effect on vessel formation, probably by acting as an artificial passive repressor and forming inactive heterodimers (Yamaguchi et al., 2008). Because the misexpression of VNI2 phenocopies the overexpression of C-terminally truncated VND7 (Figures 6 and 7), and VNI2 binds to VND proteins in vitro and possibly forms heterodimers in vivo (Figures 1 and 2; see Supplemental Figure 2 online), VNI2 is a passive repressor of the VND7 and other VND transcriptional activators.

By contrast, active repressors have intrinsic repression domains, such as the ETHYLENE-RESPONSIVE ELEMENT BINDING FACTOR (ERF)-associated amphiphilic repression (EAR) motif in plants, which might affect chromatin modification, including histone methylation and heterochromatin formation

(Kazan, 2006). Our transient reporter assays showed that full-length and C-terminally truncated VNI2 proteins significantly reduced *luc* reporter expression (Figure 5C), suggesting that VNI2 might function as an active repressor, independent of VND7 binding. It is noteworthy that we found a sequence similar to the EAR motif ($^{L}/_{F}$DLN$^{L}/_{F}$[x]P), which is conserved in class II ERFs and TFIIIA-type zinc finger proteins (Ohta et al., 2001), within the possible PEST motif (TTDLNLLPSSPSSD; the EAR motif-like sequence is underlined) in the C-terminal region of VNI2 (Figure 1B). The functional significance of the EAR motif-like sequence in VNI2 is an important issue to be clarified in future research.

Degradation of VNI2

Plants use the degradation of positive and negative regulators to optimize the signaling pathways for growth and development (reviewed in Huq, 2006). The activity of several NAC domain proteins, including NAC1 and ANAC019, is known to be regulated by ubiquitin-dependent protein degradation (reviewed in Olsen et al., 2005). We have shown that the stability of VNI2 is increased by treatment with the proteasome inhibitor MG-132 (Figure 4), and VNI2 contains a predicted PEST motif (Figure 1B), which is known to promote rapid protein degradation (Rechsteiner and Rogers, 1996). The C-terminally truncated VNI2 protein, which lacks part of the PEST motif, is more stable than full-length VNI2 (Figure 4) and repressed vessel element differentiation as effectively as did full-length VNI2 (Figures 7 and 8). We also recently demonstrated that the stability of VND7 can be regulated by protein degradation, probably mediated by proteasomes (Yamaguchi et al., 2008). Thus, the sophisticated control of vessel differentiation may require the timely degradation of these negative and positive regulators.

Function of VNI2 in Vascular Development

We have shown that overexpression of *VNI2* significantly inhibits normal vessel element differentiation (Figures 6 and 7). These defects are also observed in plants expressing dominant-negative forms of VND7, although loss of function of *VND7* does not alter xylem development (Kubo et al., 2005; Yamaguchi et al., 2008). VND7 can form homodimers and heterodimers with other VND proteins (Yamaguchi et al., 2008), suggesting that the dominant-negative forms of VND7 affect not only VND7 itself but also other VNDs. Because VNI2 effectively binds to VND1 to VND5 proteins as well as to VND7 (Figure 2), it can regulate multiple VND proteins during xylem vessel differentiation. Initiation of *VNI2* expression precedes that of *VND7* expression in roots (Figure 3; see Supplemental Figure 4A online). We previously reported that *VND1* to *VND3* are expressed preferentially in procambial cells adjacent to root meristem (Kubo et al., 2005). Therefore, in early stages of xylem vessel differentiation before the onset of *VND7* expression, VNI2 may bind to VND1 to VND3 and repress vessel-specific genes. Moreover, an in vitro binding assay suggests that VNI2 could bind not only to VND proteins but also to other NAC domain proteins (Figure 2). Therefore, it is possible that VNI2 may also regulate transcriptional activities of some other NAC domain proteins during xylem vessel differentiation.

Loss of function of *VNI2* increases the expression of genes involved in xylem vessel formation, although the mutant does not show defects in xylem development (see Supplemental Figure 7 online). ANAC041, which has the highest sequence similarity to VNI2 (Figure 1C), does not bind as effectively as VNI2 to VND7 (Figure 2B). The T-DNA insertion mutation in *ANAC041* does not affect the expression of vessel-specific genes regulated by VND7, in contrast with the *vni2* mutant (see Supplemental Figure 7 online). These data suggest that ANAC041 does not function redundantly with VNI2 in xylem vessel differentiation. Recently, the xylem-specific NAC domain protein XND1 was shown to negatively regulate xylem vessel differentiation by suppressing the expression of vessel-related genes (Zhao et al., 2008). Although *xnd1* mutants show slightly shorter xylem vessels than the wild type, patterned secondary wall deposition and autolysis in xylem vessels of the mutants occurred normally (Zhao et al., 2008), suggesting the existence of several distinct mechanisms to repress the expression of vessel-related genes, which could in turn account for why single mutations of negative regulators show only a weak phenotype.

VNI2 expression was observed in the xylem parenchyma cells surrounding mature vessel elements in inflorescence stems (Figure 3G), in which *VND7* is also expressed strongly (see Supplemental Figure 5 online), suggesting a role for VNI2 in repressing VND7 activity in these xylem parenchyma cells. The interruption of vascular bundles induces vascular regeneration (reviewed in Aloni, 1995). When the vascular bundles in the internodes of zinnia were severed, xylem parenchyma cells readily transdifferentiated into vessel elements (Nishitani et al., 2002). It is conceivable that the rapid disappearance of VNI2's repression activity against VND7 in these xylem parenchyma cells after vascular disruption ensures the quick transdifferentiation of the vessel elements.

VNI2, but not *VND*, is expressed in the phloem cells in roots and stems (Figure 3; see Supplemental Figure 3 online). In roots, the expression of *VNI2* partially overlaps that of *APL*, which promotes and inhibits phloem and xylem differentiation, respectively (Bonke et al., 2003), suggesting a cooperative function for APL and VNI2 in inhibiting vessel element differentiation in phloem. Furthermore, *VNI2* is expressed in locations as widely

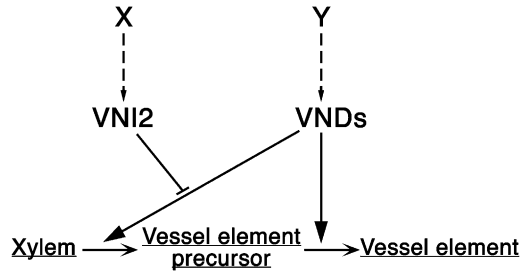

Figure 9. Schematic Model of Xylem Vessel Element Differentiation.

VNDs act as positive regulators of xylem vessel differentiation, and VNI2 represses VND function in the early stage of vessel differentiation in the roots and in xylem parenchyma cells surrounding the mature vessels in the stems. The expression of *VNDs* and *VNI2* is regulated by different developmental signals (X and Y, respectively).

separated as the shoot apical region and the guard cells (Figure 3). VNI2 may thus have pleiotropic functions in these regions or cells that are independent of its role in xylem vessel formation.

NAC Transcriptional Network Regulating Vessel Differentiation

In animals, the basic helix-loop-helix leucine zipper domain (bHLHZip) transcription factor family proteins Max, c-Myc, and Mad constitute a transcription network involved in cell proliferation, differentiation, and apoptosis by forming homodimers and heterodimers in response to upstream stimuli: c-Myc/Max and Mad/Max heterodimers act as transcriptional activators and repressors, respectively (reviewed in Lüscher, 2001; Amoutzias et al., 2008). The loss of *Arabidopsis* VND7 function produces no detectable defects in morphology (Kubo et al., 2005), and VND7 can form either homodimers or heterodimers with other VND members (Yamaguchi et al., 2008), suggesting that VND proteins function collaboratively and/or redundantly in xylem vessel differentiation. In this study, we also found that VNI2, a previously uncharacterized NAC domain transcriptional repressor, physically interacts with VND proteins. Therefore, VND proteins may well regulate xylem vessel differentiation by forming active or repressive complexes, similar to the c-Myc/Max/Mad bHLHZip transcriptional network. Moreover, as described above, XND1 was also shown to inhibit xylem vessel differentiation (Zhao et al., 2008). It is possible that VNDs, VNI2, and XND1 constitute a NAC transcriptional network that fine-tunes vessel formation-related gene expression.

Here, we identified a NAC domain protein, VNI2, which represses VND function at the early stage of vessel differentiation in roots and in the xylem parenchyma cells surrounding the mature vessels in stems (Figure 9). The differential expression pattern of *VNDs* and *VNI2* seems to be regulated by different developmental signals (Figure 9). Because the CLE peptide TDIF is a strong suppressor of vessel element differentiation (Ito et al., 2006), it will be interesting to establish whether VNI2 functions downstream of TDIF. Further analysis of VNI2, including its misexpression under the control of promoters for cell-specific genes such as *APL*, its expression during vascular regeneration, the identification of its direct targets and DNA binding sequences, and the isolation of proteins with which it interacts, will undoubtedly shed more light on the biological roles of VNI2 in vascular development.

We also proposed a novel regulatory mechanism: some NAC domain proteins interact with other NAC domain proteins to impede their functions. Such NAC–NAC interactions may play important roles in various events during plant development.

METHODS

Vector Construction

To generate the Gateway destination vectors for the expression of MBP fusion proteins in *Escherichia coli* and for the expression of proteins under the control of their own promoters in plants, pMAL-c2X (New England Biolabs) and pSMAB704 (Kubo et al., 2005) were digested with *Eco*RI and *Hin*dIII/*Sac*I, respectively, and blunted using the BKL kit (Takara Bio). These linearized fragments were ligated to *Eco*RV-digested Gateway Reading Frame Cassette (GWRFC) B (Invitrogen). The resultant plasmids were designated pMAL-GWRFC and pBG, respectively. The promoter fragments and cDNAs of *Arabidopsis thaliana* genes were amplified from genomic DNA and cDNA pools of the Columbia-0 (Col-0) ecotype by PCR with gene-specific primer sets. These fragments were subcloned into the pENTR/D-TOPO vector (Invitrogen) and then integrated into Gateway destination vectors for transformation of plants (Kubo et al., 2005), for two-hybrid assays (Yamaguchi et al., 2008), and for expression in *E. coli* (pDEST14 and pDEST17; Invitrogen) using LR Clonase (Invitrogen). The GATEWAY destination vectors containing the nucleotide sequence of the MCS fragments (Yamaguchi et al., 2008) were used as controls. For the dual luciferase transient transfection assay, p35S-GAL4-BD, the effector plasmid, and the reporter and reference plasmids containing firefly *luc* and *Renilla reniformis luc*, respectively, were prepared as described previously (Ohta et al., 2000). For the effector plasmid, p35SG, the *GUS* gene in pBI221 (Clontech) was removed and the tobacco mosaic virus sequence (Gallie et al., 1987) was inserted downstream from the *CaMV 35S* promoter (Fujimoto et al., 2000). *VND7* and *VNI2* cDNA fragments were inserted into the *Sma*I/*Sal*I sites of the p35S-GAL4-DB and p35SG effector plasmids. The promoter fragments of *LBD30*/*ASL19*/*JLO*, *MYB46*, and *XCP1* were inserted into the *Hin*dIII-blunted/*Xba*I sites of the GAL4UAS:TATA*:LUC* reporter plasmid.

Yeast Two-Hybrid Screening

Total RNA was extracted from 4-d-old *Arabidopsis* (Col-0) primary roots, and poly(A)$^+$ RNA was isolated with the GenElute mRNA Miniprep Kit (Sigma-Aldrich) according to the manufacturer's instructions. A cDNA library for two-hybrid screening was constructed with the HybriZAP-2.1 XR library construction kit (Stratagene). A budding yeast (*Saccharomyces cerevisiae*) strain AH109 (Clontech) was transformed sequentially with pGAL4-BD-VND7$^{1–143}$, which was constructed from the pGAL4BD-GWRFC vector by inserting the cDNA encoding the first 143 amino acids of VND7 by LR reaction (Yamaguchi et al., 2008) and then with the *Arabidopsis* root cDNA library. The plasmids from the positive yeast cells were isolated with the Yeastmaker yeast plasmid isolation kit (Clontech) and amplified in *E. coli*.

Phylogenetic Analysis

The deduced protein sequences of 30 NAC domain proteins were aligned with the MAFFT version 6.531b program (http://align.bmr.kyushu-u.ac.jp/mafft/online/server/) using the L-INS-i strategy. The alignment was manually optimized with the MacClade 4.08 program (Sinauer Associates). The optimized alignment around the NAC domain (110 amino acids in length; see Supplemental Data Set 1 online) was used to produce a phylogenetic tree with the MAFFT version 6.531b program (neighbor-joining method; JTT substitution model; ignoring heterogeneity among sites; 1000 bootstrap resampling). The tree was drawn with the FigTree version 1.1.2 program (http://tree.bio.ed.ac.uk/software/figtree/).

In Vitro Pull-Down Assay

VNI2 or *ANAC041* cDNAs were integrated into the pDEST17 vector (Invitrogen) and pMAL-GWRFC vector for poly-His and MBP tags, respectively. The His-VNI2 fusion protein was expressed in *E. coli* BL21-AI (Invitrogen) grown at 30°C in the presence of 0.2% (w/v) L-arabinose and then purified with Ni-agarose (Qiagen). The MBP-VNI2 and MBP-ANAC041 fusion proteins were expressed in *E. coli* BL21*trxB* (DE3; Cosmo Bio) in the presence of 0.1 mM isopropyl β-D-thiogalactoside and purified with amylase resin (New England Biolabs). *VND* and *NAC* cDNAs integrated into the pDEST14 vector (Invitrogen) were used for in vitro transcription and translation with the TNT Coupled Reticulocyte System (Promega) containing [^{35}S]Met according to the manufacturer's recommended method. The poly-His or MBP fusion proteins were immobilized

with Ni-agarose or amylase resin, respectively, and then the affinity resins were incubated with the translated products for 90 min at 4°C. The proteins retained on the resins were separated by SDS-PAGE.

Dual Luciferase Transient Transfection Assay

The effector, reporter, and reference plasmids were delivered into the rosette leaves of 4-week-old *Arabidopsis* plants by particle bombardment (GE Healthcare), and Luc activity was assayed with the Dual-Luciferase Reporter Assay System (Promega) using the Mithras LB940 (Berthold).

Plant Transformation

The resultant plasmids were electroporated into *Agrobacterium tumefaciens* strain *GV3101/pMP90*, which was used to transform *Arabidopsis* ecotype Col-0. The T1 generation of transgenic seedlings was selected on germination medium (Kubo et al., 2005) supplemented with 20 μg/mL hygromycin or 10 μg/mL vancomycin under continuous light for 7 d. The plants were transferred to antibiotic-free medium for 7 d and then planted in Jiffy 7 pots (Sakata Seed) under a 16-h-light/8-h-dark cycle. The transgenic plants, including the promoter:reporter (*YFP-NLS*, *CFP-NLS*, or *GUS*) lines, were observed according to Kubo et al. (2005) and Yamaguchi et al. (2008). The roots of the *VND7*$_{pro}$*:YFP-NLS* and the *VNI2*$_{pro}$*:YFP-NLS* plants were counterstained with propidium iodide and observed with a laser scanning confocal microscope (Zeiss LSM510 META). The inflorescence stems of the *VNI2*$_{pro}$*:GUS* plants were fixed with FAA (50 [v/v] ethanol, 10% [v/v] formaldehyde, and 5% [v/v] acetic acid) and embedded in Technovit 7100 resin (Heraeus Kulter). Sections were cut with a microtome (Leica RM2165) and counterstained with neutral red. The inflorescence stems of the *VND7*$_{pro}$*:GUS* and the *VNI2*$_{pro}$*:GUS* plants were fixed with FAA, and sections were cut with the vibratome (Zero 1; Dosaka EM) and counterstained with phloroglucinol HCl.

Fluorometric Analysis of GUS Activity

VNI2$_{pro}$*:VNI2-GUS* transgenic plants (T3 generations) were grown for 7 or 8 d on the GM plate. The *VNI2*$_{pro}$*:VNI2*^{full}*-GUS* plants were soaked with the sterilized water with or without 100 μM MG-132 (Wako Pure Chemical) for 6 h. Total protein was extracted in the extraction buffer (Yoshizumi et al., 1999). A 50-μL aliquot of extract was mixed with an equal volume of 1 mM 4-methylumbelliferyl-β-D-glucuronide in the extraction buffer and incubated for 1 h at 37°C. A 10-μL aliquot of each reaction was mixed with 1 mL of 0.2 M sodium carbonate, and the fluorescence was quantified by a Safire spectrophotometer (Tecan).

Expression Analysis

Total RNA from wild-type plants, transgenic plants, or T-DNA insertion lines was extracted using the Nucleospin RNA Plant System (Macherey-Nagel). cDNA was synthesized from the RNA with reverse transcriptase (SuperScript III; Invitrogen) and oligo(dT) primer and amplified by PCR with ExTaq DNA polymerase (Takara Bio) and primers specific for the target genes. Quantitative RT-PCR was performed in an ABI Prism 7000 sequence detection system (Applied Biosystems) using a QuantiTect SYBR Green PCR Kit (Qiagen). Primer sets used in the expression analysis are described in Supplemental Table 1 online.

Microarray analysis was performed using GeneChip ATH1 *Arabidopsis* genome arrays (Affymetrix) of three independent biological replicates from the roots of 5-d-old *35S*$_{pro}$*:YFP* and *35S*$_{pro}$*:VND7-YFP* seedlings (T3 generations), as previously described (Kubo et al., 2005). GeneSpring GX 7.3 (Agilent Technologies) was used for the data analysis. P values for differences between *35S*$_{pro}$*:YFP* and *35S*$_{pro}$*:VND7-YFP* plants were calculated by Welch's *t* test, based on a two-tailed distribution (n = 3). We calculated a *Q* value to estimate the false discovery rate from the P value described above using QVALUE software (Storey and Tibshirani, 2003) with the default setting. We considered genes with a *Q* value of <0.05 to be genes expressed at different levels in *35S*$_{pro}$*:YFP* and *35S*$_{pro}$*:VND7-YFP* plants.

In Situ Hybridization Analysis

Root explants derived from 6-d-old seedlings of *Arabidopsis* ecotype Col-0 were fixed in PBS containing 4% (w/v) paraformaldehyde. Paraffin sections were made from the fixed samples and hybridized with digoxigenin-labeled probes, followed by detection of signals using alkaline phosphatase–conjugated antidigoxigenin antibody, as described previously (Ohtani et al., 2008). Probes were prepared from cloned DNA sequences encoding the C-terminal regions of VNI2 (for primer information, see Supplemental Table 1 online).

Accession Numbers

Sequence data from this study can be found in the GenBank/EMBL data libraries under the following accession numbers: At5g09330 (*VNI1*), At5g13180 (*VNI2*), At2g33480 (*ANAC041*), At2g18060 (*VND1*), At4g36160 (*VND2*), At5g66300 (*VND3*), At1g12260 (*VND4*), At1g62700 (*VND5*), At5g62380 (*VND6*), At1g71930 (*VND7*), At2g46770 (*NST1*), At3g61910 (*NST2*), At1g32770 (*NST3*/*SND1*/*ANAC012*), At5g64530 (*XND1*), At1g01720 (*ATAF1*), At5g08790 (*ATAF2*), At1g52880 (*NAM*), At1g52890 (*ANAC019*), At1g56010 (*NAC1*), At1g69490 (*NAP*), At3g15170 (*CUC1*), At5g53950 (*CUC2*), At1g76420 (*CUC3*), At4g01540 (*NTM1*), At4g27410 (*RD26*), At4g35580 (*CBNAC*), At5g22290 (*FAN*), At5g24590 (*TIP*), At5g39610 (At *NAC6*), At5g64060 (*ANAC103*), At4g00220 (*LBD30*/*ASL19*/*JLO*), At5g12870 (*MYB46*), At4g35350 (*XCP1*), and At4g05320 (*UBQ10*). Microarray data from this article can be found at ArrayExpress (http://www.ebi.ac.uk/arrayexpress) under accession number E-MEXP-1876.

Supplemental Data

The following materials are available in the online version of this article.

Supplemental Figure 1. VNI1 Interacts with VND7.

Supplemental Figure 2. VNI2 Interacts with VND4 and VND5 Proteins and with VND7 Protein in Vitro.

Supplemental Figure 3. *VNI2* Is Expressed in Protophloem and Protoxylem.

Supplemental Figure 4. Overlapping Expression of *VNI2* and *VND7* in Roots.

Supplemental Figure 5. Expression of *VND7*$_{pro}$*:GUS* and *VNI2*$_{pro}$*:GUS* in Inflorescence Stems.

Supplemental Figure 6. Seventy-Day-Old Transgenic Plants.

Supplemental Figure 7. T-DNA Insertion Lines of the *VNI2* and *ANAC041* Genes.

Supplemental Figure 8. Expression Levels of *VND7* and Genes Downstream from VND7 in Transgenic Plants.

Supplemental Table 1. Oligonucleotides Used in This Study.

Supplemental Data Set 1. Sequences Used to Generate the Phylogenetic Tree Presented in Figure 1C.

Supplemental Data Set 2. Genes with Expression Changes of at Least Fourfold in *35S*$_{pro}$*:VND7* Transgenic Plants ($P < 0.05$, $Q < 0.05$).

Supplemental Data Set 3. Expression Levels of Vascular-Related Genes in Wild-Type and *VND7*-Overexpressing Plants.

ACKNOWLEDGMENTS

We thank Ian Smith (Nara Institute of Science and Technology, Japan) for proofreading the manuscript, Nobuyuki Nishikubo (Oji Paper, Japan) for providing technical advice for the sectioning of the inflorescence stems, Tomoyuki Nishiyama (Kanazawa University, Japan) for advice on the phylogenetic analysis, Hiromi Ogawa, Ayumi Ihara, Mitsutaka Araki, Sachiko Oyama, Tomoko Matsumoto, and Ryoko Hiroyama (RIKEN, Japan) for excellent technical assistance, and Minami Matsui, Takeshi Yoshizumi, Youichi Kondo, and Mieko Higuchi (RIKEN, Japan) for providing technical advice for the fluorometric analysis of GUS activity. This work was supported by Grants-in-Aid for Scientific Research (Grants 20770041 to M.Y. and 21027031 to T.D.) from the Ministry of Education, Culture, Sports, Science, and Technology.

Received October 28, 2008; revised March 11, 2010; accepted March 24, 2010; published April 13, 2010.

REFERENCES

Aida, M., Ishida, T., Fukaki, H., Fujisawa, H., and Tasaka, M. (1997). Genes involved in organ separation in Arabidopsis: an analysis of the cup-shaped cotyledon mutant. Plant Cell **9:** 841–857.

Aloni, R. (1995). The induction of vascular tissues by auxin and cytokinin. In Plant Hormones, Physiology, Biochemistry, and Molecular Biology, P.J. Davies, ed. (Dordrecht, The Netherlands: Kluwer Academic Publishers), pp. 531–546.

Amoutzias, G.D., Robertson, D.L., Van de Peer, Y., and Oliver, S.G. (2008). Choose your partners: Dimerization in eukaryotic transcription factors. Trends Biochem. Sci. **33:** 220–229.

Bonke, M., Thitamadee, T., Mähönen, A.P., Hauser, M.-T., and Helariutta, Y. (2003). APL regulates vascular tissue identity in *Arabidopsis.* Nature **426:** 181–186.

Brown, D.M., Zeef, L.A., Ellis, J., Goodacre, R., and Turner, S.R. (2005). Identification of novel genes in *Arabidopsis* involved in secondary cell wall formation using expression profiling and reverse genetics. Plant Cell **17:** 2281–2295.

Caño-Delgado, A., Yin, Y., Yu, K., Vafeados, D., Mora-García, S., Cheng, J.-C., Nam, K.H., Li, J., and Chory, J. (2004). BRL1 and BRL3 are novel brassinosteroid receptors that function in vascular differentiation in *Arabidopsis.* Development **131:** 5341–5351.

Carlsbecker, A., and Helariutta, Y. (2005). Phloem and xylem specification: pieces of the puzzle emerge. Curr. Opin. Plant Biol. **8:** 512–517.

Delessert, C., Kazan, K., Wilson, I.W., Van Der Straeten, D., Manners, J., Dennis, E.S., and Dolferus, R. (2005). The transcription factor ATAF2 represses the expression of pathogenesis-related genes in Arabidopsis. Plant J. **43:** 745–757.

Demura, T., and Fukuda, H. (2007). Transcriptional regulation in wood formation. Trends Plant Sci. **12:** 64–70.

Fujimoto, S.Y., Ohta, M., Usui, A., Shinshi, H., and Ohme-Takagi, M. (2000). *Arabidopsis* ethylene-responsive element binding factors act as transcriptional activators or repressors of GCC box-mediated gene expression. Plant Cell **12:** 393–404.

Fukuda, H. (2004). Signals that control plant vascular cell differentiation. Nat. Rev. Mol. Cell Biol. **5:** 379–391.

Funk, V., Kositsup, B., Zhao, C., and Beers, E.P. (2002). The Arabidopsis xylem peptidase XCP1 is a tracheary element vacuolar protein that may be a papain ortholog. Plant Physiol. **128:** 84–94.

Gallie, D.R., Sleat, D.E., Watts, J.W., Turner, P.C., and Wilson, T.M.A. (1987). The 5′-leader sequence of tobacco mosaic virus RNA enhances the expression of foreign gene transcripts *in vitro* and *in vivo.* Nucleic Acids Res. **15:** 3257–3273.

Greve, K., La Cour, T., Jensen, M.K., Poulsen, F.M., and Skriver, K. (2003). Interaction between plant RING-H2 and plant-specific NAC (NAM/ATAF1/2/CUC2) proteins: RING-H2 molecular specificity and cellular localization. Biochem. J. **371:** 97–108.

Hanzawa, Y., Takahashi, T., Michael, A.J., Burtin, D., Long, D., Pineiro, M., Coupland, G., and Komeda, Y. (2000). *ACAULIS5*, an *Arabidopsis* gene required for stem elongation, encodes a spermine synthase. EMBO J. **19:** 4248–4256.

Hawker, N.P., and Bowman, J.L. (2004). Roles for class III HD-Zip and KANADI genes in Arabidopsis root development. Plant Physiol. **135:** 2261–2270.

Hiratsu, K., Ohta, M., Matsui, K., and Ohme-Takagi, M. (2002). The SUPERMAN protein is an active repressor whose carboxy-terminal repression domain is required for the development of normal flowers. FEBS Lett. **514:** 351–354.

Huq, E. (2006). Degradation of negative regulators: A common theme in hormone and light signaling networks? Trends Plant Sci. **11:** 4–7.

Ito, Y., Nakanomyo, I., Motose, H., Iwamoto, K., Sawa, S., Dohmae, N., and Fukuda, H. (2006). Dodeca-CLE peptides as suppressors of plant stem cell differentiation. Science **313:** 842–845.

Kazan, K. (2006). Negative regulation of defence and stress genes by EAR-motif-containing repressors. Trends Plant Sci. **11:** 109–112.

Kim, H.S., Park, B.O., Yoo, J.H., Jung, M.S., Lee, S.M., Han, H.J., Kim, K.E., Kim, S.H., Lim, C.O., Yun, D.-J., Lee, S.Y., and Chung, W.S. (2007). Identification of a calmodulin-binding NAC protein as a transcriptional repressor in *Arabidopsis.* J. Biol. Chem. **282:** 36292–36302.

Kim, S.-G., Lee, A.-K., Yoon, H.-K., and Park, C.-M. (2008). A membrane-bound NAC transcription factor NTL8 regulates gibberellic acid-mediated salt signaling in Arabidopsis seed germination. Plant J. **55:** 77–88.

Ko, J.-H., Yang, S.H., Park, A.H., Lerouxel, O., and Han, K.-H. (2007). ANAC012, a member of the plant-specific NAC transcription factor family, negatively regulates xylary fiber development in *Arabidopsis thaliana.* Plant J. **50:** 1035–1048.

Kubo, M., Udagawa, M., Nishikubo, N., Horiguchi, G., Yamaguchi, M., Ito, J., Mimura, T., Fukuda, H., and Demura, T. (2005). Transcription switches for protoxylem and metaxylem vessel formation. Genes Dev. **19:** 1855–1860.

Lüscher, B. (2001). Function and regulation of the transcription factors of the Myc/Max/Mad network. Gene **277:** 1–14.

Mähönen, A.P., Bishopp, A., Higuchi, M., Nieminen, K.M., Kinoshita, K., Tömäkangas, K., Ikeda, Y., Oka, A., Kakimoto, T., and Helariutta, Y. (2006). Cytokinin signaling and its inhibitor AHP6 regulate cell fate during vascular development. Science **311:** 94–98.

Mähönen, A.P., Bonke, M., Kauppinen, L., Riikonen, M., Benfey, P. N., and Helariutta, Y. (2000). A novel two-component hybrid molecule regulates vascular morphogenesis of the *Arabidopsis* root. Genes Dev. **14:** 2938–2943.

Mitsuda, N., Iwase, A., Yamamoto, H., Yoshida, M., Seki, M., Shinozaki, K., and Ohme-Takagi, M. (2007). NAC transcription factors, NST1 and NST3, are key regulators of the formation of secondary walls in woody tissues of *Arabidopsis.* Plant Cell **19:** 270–280.

Mitsuda, N., Seki, M., Shinozaki, K., and Ohme-Takagi, M. (2005). The NAC transcription factors NST1 and NST2 of *Arabidopsis* regulate secondary wall thickenings and are required for anther dehiscence. Plant Cell **17:** 2993–3006.

Motose, H., Sugiyama, M., and Fukuda, H. (2004). A proteoglycan mediates inductive interaction during plant vascular development. Nature **429:** 873–878.

Muñiz, L., Minguet, E.G., Singh, S.K., Pesquet, E., Vera-Sirera, F., Moreau-Courtois, C.L., Carbonell, J., Blázquez, M.A., and Tuominen, H. (2008). ACAULIS5 controls *Arabidopsis* xylem specification through the prevention of premature cell death. Development **135:** 2573–2582.

Nishitani, C., Demura, T., and Fukuda, H. (2002). Analysis of early processes in wound-induced vascular regeneration using *TED3* and *ZeHB3* as molecular markers. Plant Cell Physiol. **43:** 79–90.

Ogo, Y., Kobayashi, T., Nakanishi Itai, R., Nakanishi, H., Kakei, Y., Takahashi, M., Toki, S., Mori, S., and Nishizawa, N.K. (2008). A novel NAC transcription factor, IDEF2, that recognizes the iron deficiency-responsive element 2 regulates the genes involved in iron homeostasis in plants. J. Biol. Chem. **283:** 13407–13417.

Ohta, M., Matsui, K., Hiratsu, K., Shinshi, H., and Ohme-Takagi, M. (2001). Repression domains of class II ERF transcriptional repressors share an essential motif for active repression. Plant Cell **13:** 1959–1968.

Ohta, M., Ohme-Takagi, M., and Shinshi, H. (2000). Three ethylene-responsive transcription factors in tobacco with distinct transactivation functions. Plant J. **22:** 29–38.

Ohtani, M., Demura, T., and Sugiyama, M. (2008). Differential requirement for the function of SRD2, an snRNA transcription activator, in various stages of plant development. Plant Mol. Biol. **66:** 303–314.

Olsen, A.N., Ernst, H.A., Leggio, L.L., and Skriver, K. (2005). NAC transcription factors: Structurally distinct, functionally diverse. Trends Plant Sci. **10:** 79–87.

Rechsteiner, M., and Rogers, S.W. (1996). PEST sequences and regulation by proteolysis. Trends Biochem. Sci. **21:** 267–271.

Sato, Y., Demura, T., Yamawaki, K., Inoue, Y., Sato, S., Sugiyama, M., and Fukuda, H. (2006). Isolation and characterization of a novel peroxidase gene *ZPO-C* whose expression and function are closely associated with lignification during tracheary element differentiation. Plant Cell Physiol. **47:** 493–503.

Scarpella, E., Francis, P., and Berleth, T. (2004). Stage-specific markers define early steps of procambium development in *Arabidopsis* leaves and correlate termination of vein formation with mesophyll differentiation. Development **131:** 3445–3455.

Sieburth, L.E., and Deyholos, M.K. (2006). Vascular development: The long and winding road. Curr. Opin. Plant Biol. **9:** 48–54.

Soyano, T., Thitamadee, S., Machida, Y., and Chua, N.-H. (2008). *ASYMMETRIC LEAVES2-LIKE19/LATERAL ORGAN BOUNDARIES DOMAIN30* and *ASL20/LBD18* regulate tracheary element differentiation in *Arabidopsis.* Plant Cell **20:** 3359–3373.

Storey, J.D., and Tibshirani, R. (2003). Statistical significance for genomewide studies. Proc. Natl. Acad. Sci. USA **100:** 9440–9445.

Taylor, N.G., Howells, R.M., Huttly, A.K., Vickers, K., and Turner, S. R. (2003). Interactions among three distinct CesA proteins essential for cellulose synthesis. Proc. Natl. Acad. Sci. USA **100:** 1450–1455.

Thiel, G., Lietz, M., and Hohl, M. (2004). How mammalian transcriptional repressors work. Eur. J. Biochem. **271:** 2855–2862.

Turner, S., Gallois, P., and Brown, D. (2007). Tracheary element differentiation. Annu. Rev. Plant Biol. **58:** 407–433.

Uauy, C., Distelfeld, A., Fahima, T., Blechl, A., and Dubcovsky, J. (2006). A NAC gene regulating senescence improves grain protein, zinc, and iron content in wheat. Science **314:** 1298–1301.

Xie, Q., Frugis, G., Colgan, D., and Chua, N.-H. (2000). *Arabidopsis* NAC1 transduces auxin signal downstream of TIR1 to promote lateral root development. Genes Dev. **14:** 3024–3036.

Xie, Q., Guo, H.-S., Dallman, G., Fang, S., Weissman, A.M., and Chua, N.-H. (2002). SINAT5 promotes ubiquitin-related degradation of NAC1 to attenuate auxin signals. Nature **419:** 167–170.

Yamaguchi, M., Kubo, M., Fukuda, H., and Demura, T. (2008). VASCULAR-RELATED NAC-DOMAIN7 is involved in the differentiation of all types of xylem vessels in Arabidopsis roots and shoots. Plant J. **55:** 652–664.

Yamamoto, R., Demura, T., and Fukuda, H. (1997). Brassinosteroids induce entry into the final stage of tracheary element differentiation in cultured *Zinnia* cells. Plant Cell Physiol. **38:** 980–983.

Yokoyama, A., Yamashino, T., Amano, Y., Tajima, Y., Imamura, A., Sakakibara, H., and Mizuno, T. (2007). Type-B ARR transcription factors, ARR10 and ARR12, are implicated in cytokinin-mediated regulation of protoxylem differentiation in roots of *Arabidopsis thaliana.* Plant Cell Physiol. **48:** 84–96.

Yoo, S.Y., Kim, Y., Kim, S.Y., Lee, J.S., and Ahn, J.H. (2007). Control of flowering time and cold response by a NAC-domain protein in *Arabidopsis.* PLoS One **2:** e642.

Yoshizumi, T., Nagata, N., Shimada, H., and Matsui, M. (1999). An *Arabidopsis* cell cycle-dependent kinase-related gene, *CDC2b*, plays a role in regulating seedling growth in darkness. Plant Cell **11:** 1883–1895.

Zhao, C., Avci, U., Grant, E.H., Haigler, C.H., and Beers, E.P. (2008). XND1, a member of the NAC domain family in *Arabidopsis thaliana*, negatively regulates lignocellulose synthesis and programmed cell death in xylem. Plant J. **53:** 425–436.

Zhao, C., Craig, J.C., Petzold, H.E., Dickerman, A.W., and Beers, E.P. (2005). The xylem and phloem transcriptomes from secondary tissues of the Arabidopsis root-hypocotyl. Plant Physiol. **138:** 803–818.

Zhong, R., Demura, T., and Ye, Z.-H. (2006). SND1, a NAC domain transcription factor, is a key regulator of secondary wall synthesis in fibers of *Arabidopsis.* Plant Cell **18:** 3158–3170.

Zhong, R., Lee, C., Zhou, J., McCarthy, R.L., and Ye, Z.-H. (2008). A battery of transcription factors involved in the regulation of secondary cell wall biosynthesis in *Arabidopsis.* Plant Cell **20:** 2763–2782.

Zhong, R., Richardson, E.A., and Ye, Z.-H. (2007a). The MYB46 transcription factor is a direct target of SND1 and regulates secondary wall biosynthesis in *Arabidopsis.* Plant Cell **19:** 2776–2792.

Zhong, R., Richardson, E.A., and Ye, Z.-H. (2007b). Two NAC domain transcription factors, SND1 and NST1, function redundantly in regulation of secondary wall synthesis in fibers of *Arabidopsis.* Planta **225:** 1603–1611.

Zhou, A., Wang, H., Walker, J.C., and Li, J. (2004). BRL1, a leucine-rich repeat receptor-like protein kinase, is functionally redundant with BRI1 in regulating *Arabidopsis* brassinosteroid signaling. Plant J. **40:** 399–409.